Complas

Fourth International Conference on Computational Plasticity. Fundamentals and Applications

4

Barcelona, Spain 3-6 April, 1995

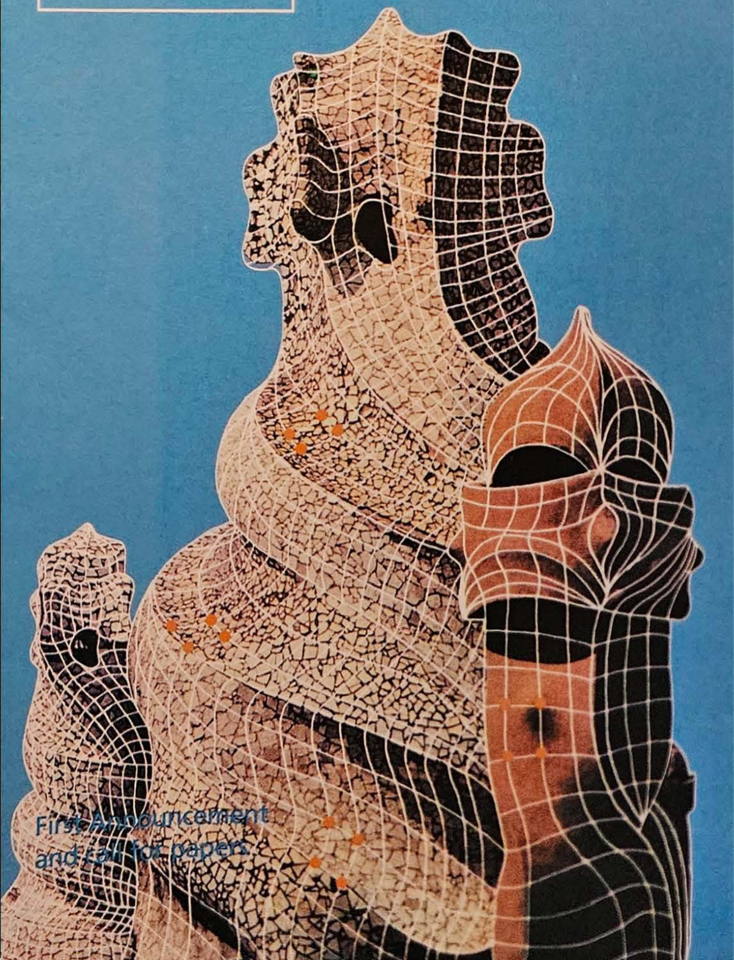

First Announcement and call for papers

Technical Advisory Panel

C. Agelet de Saracibar, Barcelona, Spain
L. Anand, Cambridge, M.A., U.S.A.
S. N. Atluri, Atlanta, U.S.A.
Z. Bazant, Chicago, U.S.A.
T. Belytschko, Chicago, U.S.A.
N. Bicanic, Swansea, U. K.
R. de Borst, Delft, Netherlands
I. Carol, Barcelona, Spain
M. Cervera, Barcelona, Spain
J. L. Chaboche, Paris, France
J. L. Chenot, Sophia Antipolis, France
M. A. Crisfield, London, U. K.
J. Doltsinis, Stuttgart, Germany
E. Dvorkin, Buenos Aires, Argentina
R. Feijoo, Rio de Janeiro, Brazil
A. Gens, Barcelona, Spain
A. Huerta, Barcelona, Spain
C. Johnson, Gotenborg, Sweden
M. Kleiber, Warsaw, Poland
B. Kröplin, Stuttgart, Germany
J. Lubliner, Berkeley, U.S.A.
G. Maier, Milan, Italy
A. Marí, Barcelona, Spain
J. B. Martin, Cape Town, South Africa
J. Miquel, Barcelona, Spain
A. Needleman, Providence, U. S. A.
J. Oliver, Barcelona, Spain
M. Ortiz, Providence, U. S. A.
M. Pastor, Cedex/UPM, Madrid, Spain
P. Perzyna, Warsaw, Poland
E. Ramm, Stuttgart, Germany
J. N. Reddy, Blacksburg, U.S.A.
C. Sagaseta, Santander, Spain
A. Samuelsson, Goteborg, Sweden
B. Schrefler, Padua, Italy
J. C. Simo, Stanford, U.S.A.
E. Stein, Hannover, Germany
B. Suárez, Barcelona, Spain
R. L. Taylor, Berkeley, U. S. A.
K. Willam, Colorado, U. S. A.
P. Wriggers, Darmstadt, Germany
G. Yagawa, Tokyo, Japan
O. C. Zienkiewicz, Swansea, U. K.

Conference Organizers:
E. Oñate, Universitat Politècnica de Catalunya, Spain
D.R.J. Owen University College of Swansea, U.K.
E. Hinton, University College of Swansea, U.K.

Conference Secretariats

Barcelona
Centro Internacional de Métodos Numéricos en Ingeniería
Módulo C1, Campus Norte UPC
Gran Capitán s/n
08034 Barcelona, Spain
Phone: 34-3/401 60 36 - 205 70 16
FAX: 34-3 / 401 65 17

Swansea
Department of Civil Engineering
University College of Swansea
Singleton Park
Swansea SA2 8PP, U.K.
Phone: 44-792 /20 56 78
FAX: 44-792 /29 56 76

Sponsors

-Comissió Interdepartamental de Recerca i Innovació Tecnològica. Generalitat de Catalunya
-Departament de Política Territorial i Obres Públiques. Generalitat de Catalunya
-Departament d'Indústria i Energia, Generalitat de Catalunya
-Dirección General de Investigación Científica y Técnica, Ministerio de Educación y Ciencia, Spain
-Escuela Técnlica Superior de Ingenieros de Caminos, Canales y Puertos, Barcelona, Spain
-European Community in Computational Methods in Applied Sciences (ECCOMAS)
-International Association for Computational Mechanics (IACM)
-International Center for Numerical Methods in Engineering, Barcelona, Spain
-International Network of Centers for Computer Applications in Engineering (INCCA)
-Sociedad Española de Métodos Numéricos en Ingeniería (SEMNI)
-UETP for Development of Numerical Methods in Engineering (COMETT Programme EEC)
-Universidad Politécnica de Catalunya (UPC)

COMPLAS IV Fourth International Conference on Computational Plasticity. Fundamentals and Applications. Barcelona, Spain 3–6 April, 1995

POST-CRITICAL STATES IN THIN SHEETS WITH LOCALIZED AND DIFFUSE PLASTIC ZONES

M. Kowalczyk, Z. Mróz
Institute of Fundamental Technological Research PAS
ul. Świętokrzyska 21, Warsaw, Poland

Abstract

In certain problems of loading of elastic-perfectly plastic thin sheets a continuous displacement solution may not exist. The evolution of plastic zone is then connected with the evolution of discontinuity lines in both velocity and displacement fields. It was assumed by Mróz and Kowalczyk [2] that in the presence of discontinuity lines the localized plastic zones start to proceed. This new failure mode was described by an additional constitutive relation between displacement discontinuity and interface traction along the material discontinuity line. In the former paper, following the complete elasto-plastic analysis of axisymmetric disks response, a limit state was reached after stable or unstable behavior. In the present paper, as an example the same problem is solved using FE method and a more realistic solution is presented in which it is assumed that the ultimate failure is caused by circumferential localization and evolution of radial cracks. In the nonlinear incremental analysis a new reliable algorithm of continuation method is developed. It is based on rank analysis of the rectangular matrix of homogeneous set of incremental equations. Theoretical background of this method is presented and numerical examples illustrate its usefulness in post-critical analysis.

1. INTRODUCTION

The present paper is concerned with analysis of elasto-plastic states in thin discs where the localized flow zones may develop simultaneously with the diffuse zones. However, the general methodology developed in this paper could be applied to any problem where the localized deformation zones develop. The problem of localized flow can be treated within large deformation theory with account for hardening and softening effects, see for instance, Tvergaard [1]. However, much simplified approach is obtained when the localized zone is treated as an interface between two elastic or elasto-plastic materials. The constitutive relations are then formulated for displacement discontinuities and interface tractions. This approach was used by Mróz and Kowalczyk [2] in the analysis of decohesion of circular disc from the inner rigid support. The radial displacement discontinuity is then related to radial stress by considering the localization mode constituted by out-of-plane shearing. The initial plastic flow is disturbed by presence of the localized zone with subsequent unloading and new plastic regimes developing. The next localization zones are expected to develop in radial directions, thus producing ultimate disc failure.

The analysis of this class of problems is associated with continuation methods which are described, for instance, by Crisfield et al. [3], Seydel [4], Rheinboldt et al. [5]. and combined with the finite element method, cf. Zienkiewicz [6], and Crisfield [7]. In this paper a new variant of continuation is presented. It is associated with the rank analysis of a rectangular set of governing equations. This method is next applied to study propagation of radial localization zones in circular discs subjected to tensile tractions.

2. LOCALIZATION ZONES TREATED AS DISCONTINUITY INTERFACES

In solving boundary-value problems for elasto-plastic disks of a perfectly plastic material, different stress regimes are encountered, namely elliptic, hyperbolic or parabolic. For elliptic stress regimes, there are no real characteristics within the disk-plane, whereas for parabolic or hyperbolic regimes there exist one or two families of stress and velocity characteristics. Velocity discontinuity may then occur along characteristics as a part of the solution. Denoting by Δv_n and Δv_t the normal and tangential velocity discontinuities and by V_n the normal velocity of propagation of the material element across the discontinuity line S_v, the discontinuity in strain components referred to a local coordinate system (n, t) is expressed as follows:

$$\Delta \varepsilon_{nn} = \frac{\Delta v_n}{V_n} \qquad \Delta \gamma_{nt} = \frac{\Delta v_t}{V_n} \qquad \Delta \varepsilon_{tt} = 0 \tag{1}$$

where the n and t axes are normal and tangential to the line S_v.

From the relations (1) it follows that when the discontinuity line moves with the material particles ($V_n = 0$), the strain discontinuity tends to infinity. Such a situation occurs in axisymmetric disks which have stepwise thickness or are rigidly constrained at one of the edges. The solution for a rigid-plastic model then exhibits normal velocity discontinuity along circumferential lines or normal displacement discontinuity in an elasto-plastic solution. Such a displacement or infinite strain discontinuity may create doubt about the physical validity of the solution.

Physically it can be expected that a localized flow zone occurs in such situations. In the presence of discontinuity lines an additional constitutive relation between the rate of displacement discontinuity and the respective traction rate along the material discontinuity line was assumed by Mróz and Kowalczyk [2]. Figure 1 presents the mode of deformation in the localized plastic zone. Two rigid material blocks are sliding along slip planes towards middle plane. Within an assumption that the normal stress distribution is uniform, from the condition of equilibrium of normal forces it follows

$$\sigma_n = \sigma^* \left(1 - \frac{2}{H} \| d_n \|\right) \tag{2}$$

where $\| d_n \|$ describes displacement jump across plastic decohesion zone, H denotes thickness and $\sigma^* = \sigma_0/\sqrt{1-\nu+\nu^2}$ (σ_0 is the yield stress). On the other hand, the usual flow rule occurs within domains of regular solution.

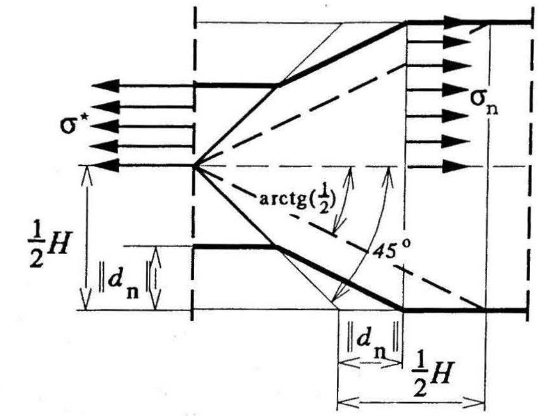

Figure 1: Mode of deformation in the localized zone

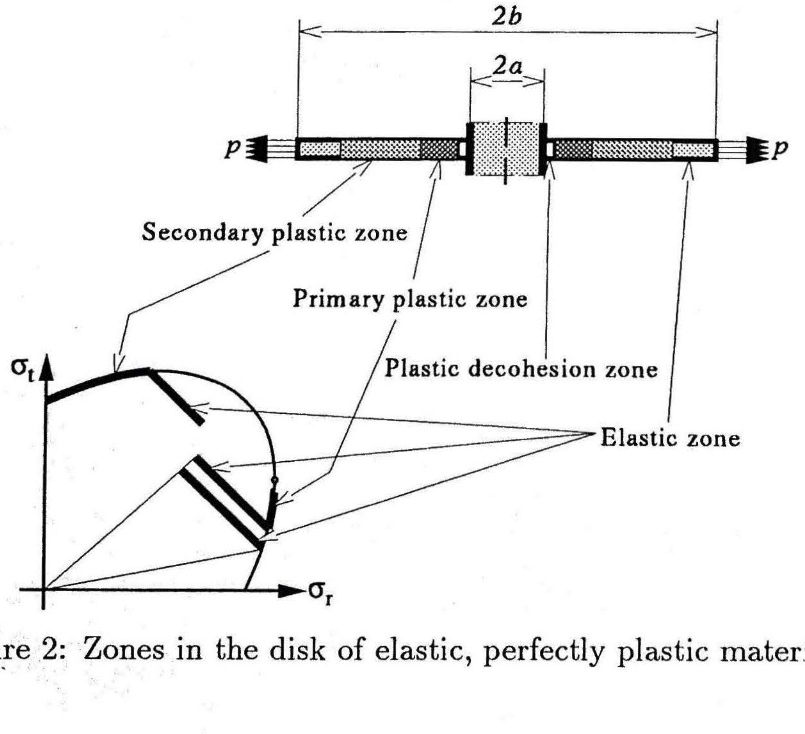

Figure 2: Zones in the disk of elastic, perfectly plastic material

In the case of axisymmetric disk problem and for a perfectly plastic material model, the plastic decohesion process causes structural softening with very complicated stable or unstable post-critical response. Figure 2 presents different zones within loaded structure and typical three consecutive stress paths in the stress plane. A limit state was reached after the complete elasto-plastic analysis for both Tresca and Huber-Mises yield conditions. In the present paper, as an example the same problem is solved using FE method and a more realistic solution is presented in which it is assumed that the ultimate failure is caused by the evolution of radial localization zones which subsequently become the radial cracks.

3. CONTINUATION METHODS IN NON-LINEAR PROBLEMS

In this section, we shall briefly discuss a new version of the continuation method associated with the rank analysis of a rectangular matrix.

3.1 Control variables in a non-linear problem

Denote by $\boldsymbol{r}$ the vector of state variables r_n $(n = 1, \ldots, N)$ in the N-dimensional Euclidean space $\mathcal{E}^N$, and by $\boldsymbol{\Gamma}$ the vector field specified by continuous and differentiable functions $\Gamma_m(\boldsymbol{r})$ $(m = 1, \ldots, M$ and $M = N - 1)$. Consider the solution of a set of non-linear algebraic equations

$$\boldsymbol{\Gamma}(\boldsymbol{r}) = 0 \tag{3}$$

Assume a particular solution of (3) specified by the vector $\boldsymbol{r}_\nu$ to be known. Moreover, let $L = N - K$ $(K \geq 1)$ equations (3) be independent for $\boldsymbol{r} = \boldsymbol{r}_\nu$. Geometrically, the set (3) can be interpreted as representing M surfaces with the solution belonging to their K-dimensional intersection. For $K = 1$, the solution of a non-linear problem (3) is represented by a curve $\mathcal{S} \in \mathcal{E}^N$, Fig.3.

Usually, the vector components r_n are divided into independent (or control) components $r_{i_k} \equiv p_k$ and dependent (or response) components $r_{i_l} \equiv u_l$, where $i_k \in <1, N>$, $k = 1, \ldots, K$; $i_l \in <1, N>$, $l = 1, \ldots, L$ and $i_k \neq i_l$. Denote by $\boldsymbol{p}$ and $\boldsymbol{u}$ the vectors constituted of independent and dependent components p_k and u_l. The solution of (3) can now be presented in the form

$$\boldsymbol{u} = \boldsymbol{\Psi}(\boldsymbol{p}) \tag{4}$$

The implicit function theorem, cf. Seydel [4], or Sikorski [8] provides the conditions for existence and uniqueness of the unknown vector function $\boldsymbol{\Psi}$ in the neighborhood of a point representing the solution $\boldsymbol{r} = \boldsymbol{r}_\nu$. Also the rule of specification of partial derivative $\partial\boldsymbol{\Psi}/\partial\boldsymbol{p}$ follows from this theorem, therefore the implicit function theorem provides the analytical background for the continuation methods.

The incremental approach will provide the ordered set $\boldsymbol{r}_\nu, \boldsymbol{r}_{\nu+1}, \ldots$ of solutions of (3) by using the relation $\boldsymbol{r}_{\nu+1} = \boldsymbol{r}_\nu + \Delta\boldsymbol{r}_\nu$. In order to determine the secant vector $\Delta\boldsymbol{r}_\nu$, different decompositions into $\Delta\boldsymbol{u}$ and $\Delta\boldsymbol{p}$ can be applied. If the respective vector function $\boldsymbol{\Psi}$ exists, then the tangential vector $\delta\boldsymbol{r}_\nu$ follows from the increments $\delta\boldsymbol{p}_\nu$ and $\delta\boldsymbol{u}_\nu$, where $\delta\boldsymbol{u}_\nu$ are uniquely specified in terms of increments $\delta\boldsymbol{p}_\nu$, i.e. $\delta\boldsymbol{u}_\nu = (\partial\boldsymbol{\Psi}/\partial\boldsymbol{p})\delta\boldsymbol{p}_\nu$. Further corrections from $\delta\boldsymbol{r}_\nu$ to $\Delta\boldsymbol{r}_\nu$ are based on the analysis of a linear set of equations, which is therefore fundamental for continuation methods.

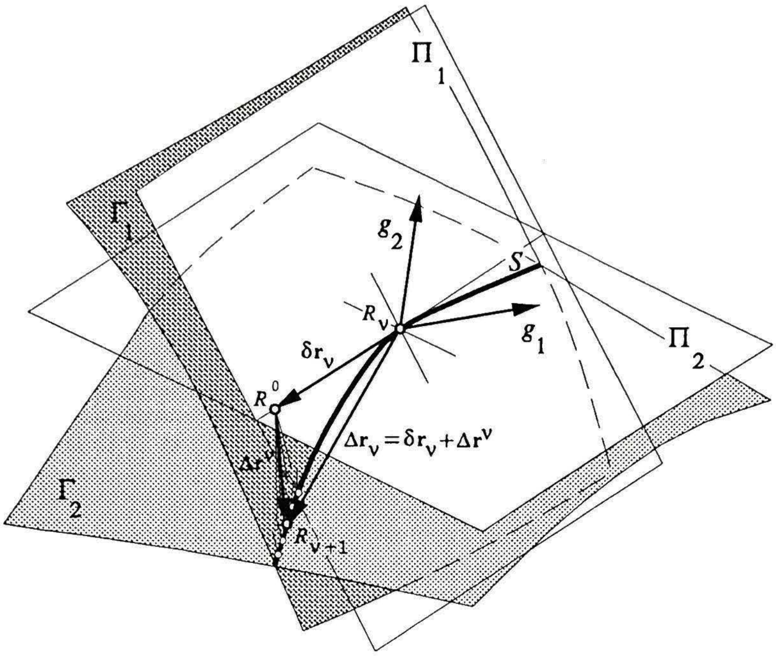

Figure 3: Geometrical interpretation of continuation procedure

3.2 Solution of homogeneous set of linear equations

Consider a set of M linear equations with M unknowns

$$\boldsymbol{A}\boldsymbol{x} = \boldsymbol{y} \tag{5}$$

This set can be rewritten in an equivalent form

$$\left.\begin{aligned} \boldsymbol{A}\boldsymbol{x} - \boldsymbol{y}x_N &= \boldsymbol{0} \\ x_N &= 1 \end{aligned}\right\} \tag{6}$$

by introducing one additional unknown x_N. Denoting by $\tilde{\boldsymbol{A}}$ the rectangular matrix $[\boldsymbol{A}, -\boldsymbol{y}]$, and by $\tilde{\boldsymbol{x}}$ the vector $[\boldsymbol{x}^T, x_N]^T$ of $N = M + 1$ components, the first set of eqs. (6) can be written as follows

$$\tilde{\boldsymbol{A}}\tilde{\boldsymbol{x}} = \boldsymbol{0} \tag{7}$$

The homogeneous set of equations can be solved to within a scalar parameter. In fact, if a given non-zero vector $\tilde{\boldsymbol{x}}^*$ satisfies (7), then any vector

$$\tilde{\boldsymbol{x}} = \kappa\tilde{\boldsymbol{x}}^* \tag{8}$$

also satisfies (7). It is seen that the condition $x_N = 1$ implies the normalization procedure providing $\kappa = 1/x_N^*$ and the solution $\tilde{\boldsymbol{x}}$ is specified. Thus the solution of (6) is obtained by generating the solution of the homogeneous set of (7) with subsequent scaling according to (8). Let us now discuss the procedure of generating $\tilde{\boldsymbol{x}}^*$ (the star superscript will be omitted in the subsequent formulae).

In the case of a homogeneous set (7) the rank of $\tilde{\boldsymbol{A}}$ is lower than the number of unknowns, thus $r = \text{rank}(\tilde{\boldsymbol{A}}) < N$. A non-trivial solution $\tilde{\boldsymbol{x}}$ then always exists, cf. [9, 10]. Decompose the vector $\tilde{\boldsymbol{x}}$ into $\boldsymbol{p}$ and $\boldsymbol{u}$, where $\boldsymbol{p}$ and $\boldsymbol{u}$ are vectors with K independent (control) and L dependent (response) components. The set of equations (7) can be presented as a non-homogeneous set in the form

$$\boldsymbol{U}\boldsymbol{u} = -\boldsymbol{P}\boldsymbol{p} \tag{9}$$

where $\boldsymbol{U}$ is a square matrix $(L \times L)$, and $\boldsymbol{P}$ is constituted by the same rows as the matrix $\boldsymbol{U}$ and the columns of $\tilde{\boldsymbol{A}}$ which do not occur in $\boldsymbol{U}$.

The selection of the regular matrix $\boldsymbol{U}$ is not unique, and the additional condition should be set in order to provide optimal selection of $\boldsymbol{U}$. Starting with $L = M$, we require the matrix $\boldsymbol{U}$ to be non-singular and characterized by a maximal value of its determinant among all matrices of the same size, thus

$$\det(\boldsymbol{U}) = \max \qquad \text{for } \boldsymbol{U} \in \boldsymbol{U}^* \tag{10}$$

where $\boldsymbol{U}^*$ denotes the set of all square $(L \times L)$ matrices generated from the rectangular matrix $\tilde{\boldsymbol{A}}$. When $\det(\boldsymbol{U}) \to 0$, the size of the matrix is lowered until $L = r$. A more sensitive criterion for rank evaluation is provided by the matrix condition number specified as the ratio of maximal and minimal eigenvalues. When all eigenvalues are positive, then for vanishing of one eigenvalue we have $\det(\boldsymbol{U}) \to 0$ and $\text{cond}(\boldsymbol{U}) \to \infty$. Thus the large value of $\text{cond}(\boldsymbol{U})$ indicates the necessity of transition to the matrix of lower size. The condition number can be calculated by following the algorithm presented in [9] without necessity of solving eigenvalue problem.

A non trivial solution $\tilde{\boldsymbol{x}}$ is obtained by solving the set (9) for arbitrary selected component values of the control vector $\boldsymbol{p}$. In particular, when $r = M$, the orientation of the vector $\tilde{\boldsymbol{x}}$ depends on one parameter, say $p_1 = 1$, and is unique. When $r < M$, the orientation of the vector $\tilde{\boldsymbol{x}}$ is not unique. We can construct a set of K independent vectors $\boldsymbol{p}_i$ assuming $(p_k)_i = \delta_{ik}$ $(i, k = 1, \ldots, K;\ \delta_{ik} = 1$ for $i = k$ and $\delta_{ik} = 0$ for $i \neq k)$ and determine fundamental solutions $\tilde{\boldsymbol{x}}_i$ composed of the vectors $\boldsymbol{p}_i$ and the respective vectors $\boldsymbol{u}_i$, obtained from (9). Their linear combination provides a solution of the homogeneous set (7) and after scaling procedure, the solution of the set (5) is generated.

3.3 Control Variable Selection Method

The incremental solution of non-linear problem is associated with the linear set of equations, with proper decomposition of state vector into dependent and independent components.

Assume that ν solution points were obtained. The consecutive point $R_{\nu+1}$ is obtained through the iterative procedure in two steps

$$\left.\begin{array}{lrl} \text{predictor:} & \boldsymbol{r}^0 = & \boldsymbol{r}_\nu + \delta\boldsymbol{r}_\nu \\ \text{corrector:} & \boldsymbol{r}^{k+1} = & \boldsymbol{r}^k + \delta\boldsymbol{r}^k \end{array}\right\} \tag{11}$$

where $\boldsymbol{r}^k$ denotes k-th approximation of the vector $\boldsymbol{r}_{\nu+1}$. When the condition $|\Gamma_m(\boldsymbol{r}^k)| \leq \varepsilon$ is satisfied (ε is a specified solution accuracy), the iterative process is stopped, and we assume

$$\boldsymbol{r}_{\nu+1} := \boldsymbol{r}^k = \boldsymbol{r}_\nu + \Delta\boldsymbol{r}_\nu = \boldsymbol{r}_\nu + \delta\boldsymbol{r}_\nu + \sum_{j=0}^{k-1} \delta\boldsymbol{r}^j \tag{12}$$

Otherwise, the consecutive term $\delta\boldsymbol{r}^k$ is calculated. The function $\Gamma_m(\boldsymbol{r}^k)$ is represented by the Taylor series near $\boldsymbol{r} = \boldsymbol{r}^k$, thus

$$\frac{\partial\Gamma_m(\boldsymbol{r}^k)}{\partial\boldsymbol{r}}\delta\boldsymbol{r}^k + \Theta_m(\boldsymbol{r}^k) = \Gamma_m(\boldsymbol{r}^{k+1}) - \Gamma_m(\boldsymbol{r}^k) \tag{13}$$

It is assumed that $\Theta_m(\boldsymbol{r}^k) \cong 0$ and $\Gamma_m(\boldsymbol{r}^{k+1}) \cong 0$, so eqs. (13) can be written in the form

$$\boldsymbol{G}\delta\boldsymbol{r}^k = -\boldsymbol{\Gamma}(\boldsymbol{r}^k) \tag{14}$$

where $\boldsymbol{G}$ denotes the gradient matrix $\partial\boldsymbol{\Gamma}/\partial\boldsymbol{r}$.

In the predictor step, the right hand side vector in the above set of equations can be neglected according to the condition $|\Gamma_m(\boldsymbol{r}_\nu)| \leq \varepsilon$. It means that the increment vector $\delta\boldsymbol{r}_\nu$ is assumed to be parallel to the unit tangent vector $\dot{\boldsymbol{r}}$ lying on the edge of intersection of tangent planes Π_m, Fig.3. The solution calculated at R_ν from the homogeneous set $\boldsymbol{G}\dot{\boldsymbol{r}} = 0$ provides $\dot{\boldsymbol{r}}_\nu$ and thus the increment $\delta\boldsymbol{r}_\nu = \kappa\dot{\boldsymbol{r}}_\nu$ is obtained to within a scaling factor κ. This factor can be evaluated from the assumed increment step length.

In the corrector step, we have $|\Gamma_m(\boldsymbol{r}^k)| > \varepsilon$. and the inhomogeneous set (14) with the rectangular matrix should be solved. To obtain a square matrix, usually an additional equation

$$\boldsymbol{c}\delta\boldsymbol{r}^k = 0 \tag{15}$$

is added to set (14), where $\boldsymbol{c}$ denotes an auxiliary vector, cf. [4, 11]. Numerous corrector schemes can be generated in this way and their efficiency is manifested by varying positions of the solution point $R_{\nu+1}$, Fig.3. The full corrector scheme can be written in the form (5) with the matrix $\boldsymbol{A}$ and the vectors $\boldsymbol{x}$, $\boldsymbol{y}$ in the form

$$\boldsymbol{A} = \begin{bmatrix} \boldsymbol{G} \\ \boldsymbol{c} \end{bmatrix} \qquad \boldsymbol{x} = \delta \boldsymbol{r}^k \qquad \boldsymbol{y} = \begin{bmatrix} -\boldsymbol{\Gamma}(\boldsymbol{r}^k) \\ 0 \end{bmatrix} \tag{16}$$

It follows from the linear algebra that the corrector scheme may fail when $\text{rank}(\boldsymbol{A}) < N$. This may occur when the vector $\boldsymbol{c}$ is linearly dependent on $\boldsymbol{G}$ or the rank of $\boldsymbol{G}$ is reduced at $\boldsymbol{r} = \boldsymbol{r}^k$.

The set of (14) can also be presented in a homogeneous form (7), where $\tilde{\boldsymbol{A}} = [\boldsymbol{G}, \boldsymbol{\Gamma}(\boldsymbol{r}^k)]$ and $\tilde{\boldsymbol{x}}^T = [(\delta \boldsymbol{r}^k)^T, x_{N+1}]$. As previously, the introduction of x_{N+1} requires proper scaling after obtaining a solution of the homogeneous set. The predictor and corrector schemes now have the same structure and the rank analysis of rectangular matrix assures the reliable solution procedure. The inequality $r < N$ implies existence of a non-trivial solution vector $\tilde{\boldsymbol{x}}$ which in view of $K \geq 2$ is always non-unique. Among the available solutions $\tilde{\boldsymbol{x}}$ the actual solution is selected so that $x_{N+1} = 1$.

4. APPLICATION TO POST-CRITICAL ANALYSIS IN THIN SHEETS

The control variable selection method can now be applied to a non-linear analysis of structures. In this paper, the problem of propagation of radial localization zones in the circular disk subjected to tensile tractions will be numerically treated using finite element discretization. The plane stress assumption are used in the analysis.

4.1 Finite element formulation

Denoting by $\boldsymbol{w}$ the nodal displacements, the displacements $\boldsymbol{d}$ and strain $\boldsymbol{\varepsilon}$ of any disk point is presented in the form

$$\boldsymbol{d} = \boldsymbol{N}\boldsymbol{w} \qquad \boldsymbol{\varepsilon} = \boldsymbol{B}\boldsymbol{w} \tag{17}$$

Further, considering only one parameter loading $\boldsymbol{f} = \lambda \boldsymbol{f}^*$, where $\boldsymbol{f}$ denotes the external tractions, λ is the load factor, and $\boldsymbol{f}^*$ is the reference loading, we have $\boldsymbol{r} = [\boldsymbol{w}^T, \lambda]^T$. Analogously to the algebraic equations (3), the equilibrium equations of a discretized structure are

$$\boldsymbol{\Gamma}(\boldsymbol{r}) = \int_V \boldsymbol{B}^T \boldsymbol{\sigma} dV - \lambda \boldsymbol{f}^* = \boldsymbol{P}(\boldsymbol{w}) - \lambda \boldsymbol{f}^* = \boldsymbol{0} \tag{18}$$

Using the virtual work equation, the following incremental equations are obtained for the corrector step

$$\boldsymbol{K} \delta \boldsymbol{w}^k = \delta \lambda^k \boldsymbol{f}^* + \boldsymbol{\theta}^k \tag{19}$$

where θ^k denotes the non-equilibrated force term and K denotes the global tangent stiffness matrix obtained from the stiffness matrices of particular elements

$$K_e = \int_{V_e} B^T \tilde{D} B dV_e \tag{20}$$

where $\tilde{D}$ denotes the tangent material stiffness matrix. Comparing (14) with (19), we have $G = [K\ ,\ -f^*]$ and $\theta^k = -\Gamma(r^k)$.

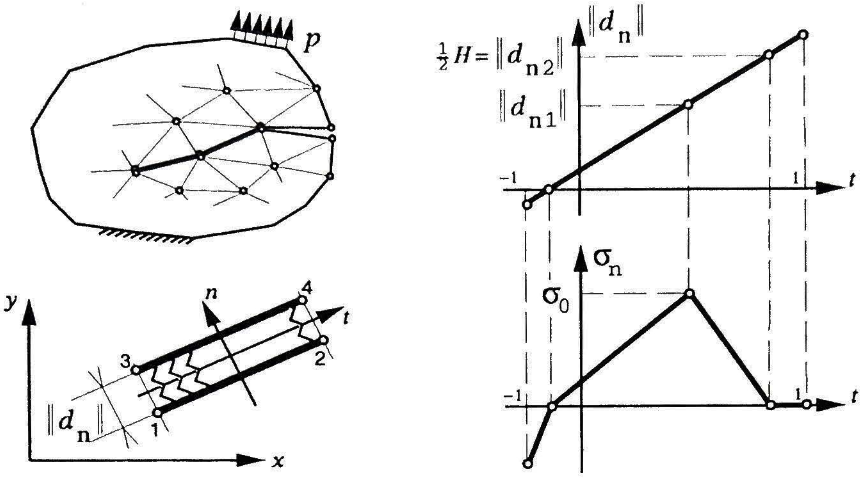

Figure 4: Finite element model and material characteristic within interface element

4.2 Diffuse plastic zone

Assuming the Huber-Mises yield condition and the associated flow rule, the stiffness matrix for a perfectly plastic material model is of the form

$$\tilde{D} = D \left(I - \frac{\left(\frac{\partial \mathcal{F}}{\partial \sigma}\right)^T \frac{\partial \mathcal{F}}{\partial \sigma} D}{\frac{\partial \mathcal{F}}{\partial \sigma} D \left(\frac{\partial \mathcal{F}}{\partial \sigma}\right)^T} \right) \qquad D = \frac{E}{1-\nu^2} \begin{bmatrix} 1 & \nu & 0 \\ \nu & 1 & 0 \\ 0 & 0 & \frac{1-\nu}{2} \end{bmatrix} \tag{21}$$

Here $\mathcal{F}(\sigma) = \sqrt{\sigma_x^2 - \sigma_x\sigma_y + \sigma_y^2 + 3\sigma_{xy}^2} - \sigma_0$, and D denotes elasticity matrix. The simplest 3-node uniform strain elements are used in specifying the plastic zones within the disk.

4.3 Interface elements used in localization zones

The localization zone is modelled as a thin interface for which the displacement rate discontinuities $\| \dot{d}_n \|$, $\| \dot{d}_t \|$ are related to contact stresses at the interface, thus

$$\| \dot{d}_n \| = \frac{\dot{\sigma}_n}{E_n} + \dot{\lambda}\frac{\partial F_c}{\partial \sigma_n} \qquad \| \dot{d}_t \| = \frac{\dot{\tau}_n}{G_n} + \dot{\lambda}\frac{\partial F_c}{\partial \tau_n} \tag{22}$$

where $F_c(\sigma_n, \tau_n)$ is the interface yield condition, $E_n = E_n^+$ for $\sigma_n > 0$, $E_n = E_n^-$ for $\sigma_n < 0$, and G_n are the elastic moduli of interface, and $\dot{\lambda} > 0$ is the plastic multiplier. However in our analysis, we set $G_n \rightarrow \infty$ and $F_c = F_c(\sigma_n)$, so the tangential discontinuity is neglected and only opening mode is studied. To avoid penetration of the interface element into the adjacent material, the compressive interface modulus E_n^- was assumed much larger then the tensile modulus E_n^+. The 4-node contact elements were used at the interface which was assumed to be material surface. The softening rule (2) was assumed between the normal traction and the interface opening $\| d_n \|$, Fig.1. When $\| d_n \| > \frac{1}{2}H$, the normal stress vanishes and the interface opening occurs. The softening response of contact elements is presented in Fig.4.

5. NUMERICAL EXAMPLES

The annular disks were considered with free inner edge $r = a$ and tensile traction p applied at the outer edge $r = b$. The reference stress is $p^* = \sigma_0$. The localization zones were assumed to follow the radial lines. However, their number is not specified from the analysis and must be assumed . The following material and geometric parameters were assumed: $E = 2.1 \times 10^5 MPa$, $\sigma_0 = 500 MPa$, $\nu = 0.3$, $a = 0.05m$, $b = 0.20m$, $H = 0.001m$.

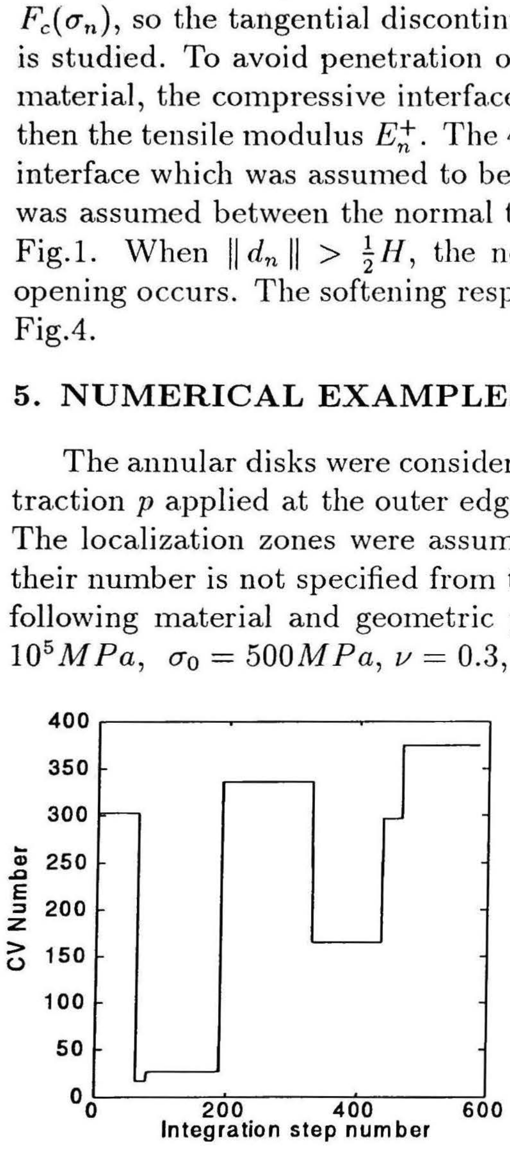

Figure 5: Numbers of selected control parameters in terms of integration step number

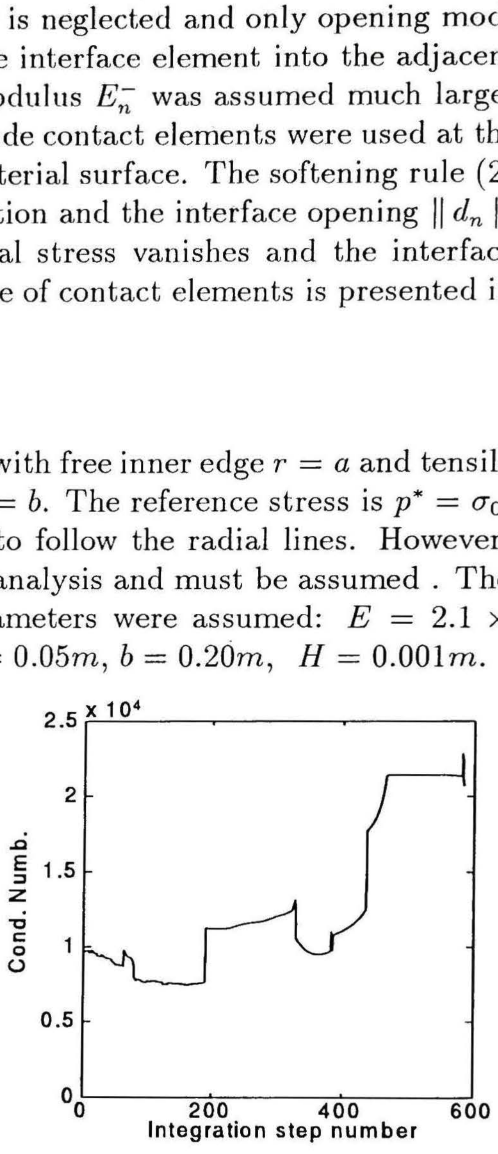

Figure 6: Condition number versus integration step number

Figures 5 and 6 present the results obtained for assumed $c = 2$ localization zones propagating along one radial line. In view of symmetry condition, only one quarter of disk was analyzed. In Figure 5 the numbers of the control vector components are shown in the course of solution process. Figure 6 presents the variation of condition number. It is seen that when the control vector component is changed, the condition number varies discontinuously. The stress and displacement limit points are traversed easily since in the present procedure they behave as regular points.

Figure 7 presents the effect of number c of localization zones on the response curve of load factor versus displacement of the node lying on the outer disk edge and symmetry axis. As it is seen, when the number c of localization zones increases, the required load level and displacements are higher. For $c = 2$, both snap-through and snap-back effects occur and the process is not controllable by external tractions and displacements. The complex stress redistribution occurs within the disk during propagation of the localized zones.

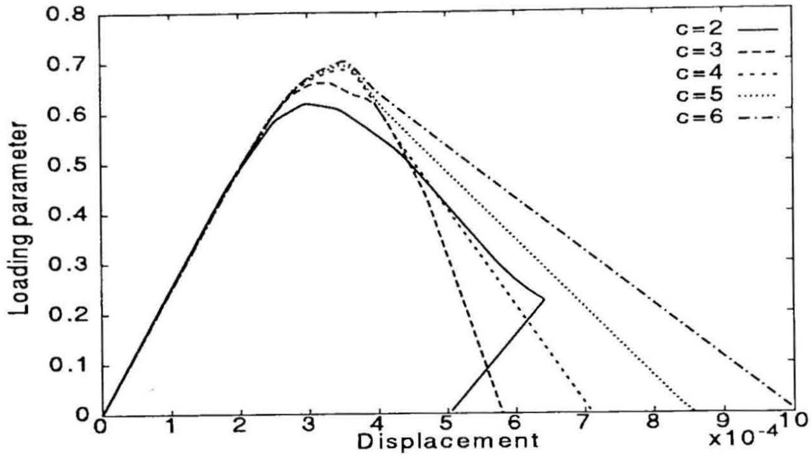

Figure 7: Influence of decohesive crack number

6. CONCLUSIONS

In the analysis of elasto-plastic behavior in the presence of discontinuity lines, an additional constitutive relation between displacement discontinuity and interface traction along the material discontinuity lines is required. Both geometric necking and material hardening or softening can be incorporated into the localized discontinuity mode. As the large displacements are confined to plastic decohesion zone, the whole analysis can be performed within small strain theory and is relatively inexpensive. Ultimate failure caused by the evolution of radial cracks leads to total collapse of the disk through a complex elasto-plastic deformation process.

The procedure of solution of linear set of equations based on rank analysis of a homogeneous set has significant advantages, namely: i) it allows to avoid computational difficulties associated with singularity or ill-conditioning of the initial square matrix of a non-homogeneous system, ii) it provides automatic selection of control variable in the analysis of non-linear problems, iii) the resulting algorithm is the same for both predictor and corrector stages. Using the control variable selection method, the turning points disappear in the numerical procedure. The bifurcation points could be treated similarly, as it was shown in [11, 12]. This method requires further improvements, especially in normalizing the square matrix in order to remove discontinuous variation of the condition number at switching control points.

References:

1. TVERGAARD, V. Necking in tensile bars with rectangular cross-section. Computer Methods in Applied Mechanics and Engineering, 103, 273-290, 1993.

2. MRÓZ, Z. and KOWALCZYK, M. Elasto-plastic post-critical analysis of disks under tension. Arch. Mech., 41, 461-480, 1989.

3. CRISFIELD, M. A. and SHI, J. A review of solution procedures and path-following techniques in relation to the non-linear finite element analysis of structures. In: P. Wriggers and W. Wagner, editors, *Nonlinear Computational Mechanics. State of the Art.* , Springer-Verlag, 47-68, 1991.

4. SEYDEL, R. *From Equilibrium to Chaos. Practical Bifurcation and Stability Analysis*, Elsevier, 1988.

5. RHEINBOLDT, W. C., ROOSE, D. and SEYDEL, R. Aspects of continuation software. In: D. Roose et al., editors, *Continuation and Bifurcations: Numerical Techniques and Applications*, Kulwer Academic Publishers, 261-268, 1990.

6. ZIENKIEWICZ, O. C. and TAYLOR, R. L. *The Finite Element Method,* McGraw-Hill, 1991.

7. CRISFIELD, M. A. *Non-linear Finite Element Analysis of Solids and Structures; Volume 1: Essentials,* John Wiley & Sons, 1991.

8. SIKORSKI, R. *Differential and Integral Calculus; Functions of Many Variables,* (in Polish) PWN, 1977.

9. FORSYTHE, G. E., MALCOLM, M. A. and MOLER, C. B. *Computer Methods for Mathematical Computations,* Prentice-Hall, 1977.

10. GOLUB, G. H. and VAN LOAN, C. F. *Matrix Computations,* Johns Hopkins University Press, 1985.

11. KOWALCZYK, M. Analysis of post-critical states in elastic and inelastic systems, (in Polish) Prace IPPT PAN, 1/94.

12. KOWALCZYK, M. Rank analysis of rectangular matrix as an element of continuation method. Engng. Comput., 10, 61-80, 1993.